The Journal of Experimental Biology 216, 1616-1623

doi:10.1242/jeb.080861

RESEARCH ARTICLE

Molecular and functional characterization of hemocyanin of the giant African millipede, *Archispirostreptus gigas*

Christian Damsgaard[1], Angela Fago[1], Silke Hagner-Holler[2], Hans Malte[1], Thorsten Burmester[3] and Roy E. Weber[1,*]

[1]Zoophysiology, Deparment of Bioscience, Aarhus University, DK 8000, Aarhus, Denmark, [2]Institute of Zoology, Molecular Animal Physiology, University of Mainz, Germany and [3]Institute of Zoology and Zoological Museum, University of Hamburg, D-20146 Hamburg, Germany

*Author for correspondence (roy.weber@biology.au.dk)

SUMMARY

In contrast to other terrestrial arthropods, where gaseous O_2 that fuels aerobic metabolism diffuses to the tissues in tracheal tubes, and most other metazoans, where O_2 is transported to tissues by circulating respiratory proteins, the myriapods (millipedes and centipedes) strikingly have tracheal systems as well as circulating hemocyanin (Hc). In order to elucidate the evolutionary origin and biological significance of millipede Hc, we report the molecular structure (subunit composition and amino acid sequence) of multimeric (36-mer) Hc from the forest floor-dwelling giant African millipede *Archispirostreptus gigas* and its allosteric oxygen-binding properties under various physico-chemical conditions. *Archispirostreptus gigas* Hc consists of only a single subunit type with differential glycosylation. Phylogenic analysis revealed that millipede Hc is a sister group to centipede HcA, which supports an early divergence of distinct Hc subunits in myriapods and an ancient origin of multimeric Hcs. *Archispirostreptus gigas* Hc binds O_2 with a high affinity and shows a strong Bohr effect. O_2 binding is, moreover, modulated by Ca^{2+} ions, which increase the O_2 affinity of the Hc in the tense (T; deoxygenated) as well as the relaxed (R; oxygenated) states, and by (L)-lactate, which modulates Hc–O_2 affinity by changing the allosteric equilibrium constant, *L*. Cooperativity in O_2 binding at half O_2 saturation (n_{50}) is pH dependent and maximal at ~pH 7.4, and the number of interacting O_2-binding sites (q) is markedly increased by binding Ca^{2+}. The data are discussed in the light of the mutually supplementary roles of Hc and the tracheal system for tissue O_2 supply.

Supplementary material available online at http://jeb.biologists.org/cgi/content/full/216/9/1616/DC1

Key words: phylogeny, oxygen binding, Diplopoda, allosteric regulation, calcium, lactate.

Received 2 October 2012: Accepted 13 January 2013

INTRODUCTION

The size and complexity of metazoan animals compelled the evolution of specific anatomical and molecular traits (notably circulatory systems and O_2-transporting proteins) to secure the transfer of O_2 from the respiratory surfaces to the respiring tissues to support aerobic metabolism. In contrast to the vast majority of animals, in which O_2 is transported by respiratory proteins such as hemoglobin (Hb), hemocyanin (Hc) and hemerythrin circulating in body fluids, terrestrial arthropods possess a tracheal system that permits gaseous diffusion of O_2 to individual tissue cells (Keilin and Wang, 1946). In this regard, the Myriapoda – which includes centipedes (class Chilopoda) and millipedes (class Diplopoda) – are of particular interest in having trachea as well as Hc (Rajulu, 1969; Mangum et al., 1985; Kusche and Burmester, 2001; Kusche et al., 2002). In contrast to Hbs, which are widely distributed in the animal kingdom, the copper-containing Hcs are extracellular proteins found only in arthropods (recorded in all subphyla) (Burmester, 2001) and molluscs (Mangum et al., 1985). However, the Hcs of these two phyla are not related but emerged independently (Burmester, 2001). Arthropod Hcs are highly multimeric. Myriapod Hcs are 6×6, 36-mer structures (Jaenicke et al., 1999) composed of up to four different subunit types (Markl et al., 2009). Each subunit consists of ~650 amino acid residues that are distributed among three structural domains and include six highly conserved histidines, which coordinate two copper (I) ions that reversibly bind one O_2 molecule (Terwilliger, 1998; Markl and Decker, 1992). The multimerization increases the O_2 transport capacity of the hemolymph without markedly raising its osmotic pressure.

As with Hbs, Hcs are allosteric proteins that are in equilibrium between two conformational states (Wyman, 1969): a tense (T) state with a low O_2 equilibrium association constant (K_T), and a relaxed (R) state with a high O_2 equilibrium association constant (K_R) (Loewe, 1978). When P_{O_2}, and thus O_2 saturation, is high (at the respiratory surfaces), most Hc molecules are in the R state, which favors O_2 loading to the hemolymph. At low P_{O_2} (as in the working muscle), the molecules are predominantly in the T state, which enhances unloading. Hc–O_2 binding is allosterically modulated by homotropic interactions (between O_2-binding sites) and heterotropic interactions (between the sites for binding O_2 and effectors) (Bonaventura and Bonaventura, 1980; Brouwer and Serigstad, 1989; van Holde et al., 2001). Heterotropic effectors modulate O_2 affinity by stabilizing or destabilizing the T and/or the R state or by altering the T–R allosteric equilibrium constant between the two protein conformations, *L*.

In contrast to the intensively studied erythrocytic vertebrate Hbs, where protons, organic phosphates and chloride ions decrease Hb–O_2

affinity by lowering K_T, striking variation is encountered amongst the multimeric invertebrate O_2-binding proteins, where effectors, commonly divalent cations, may increase or decrease K_T and/or K_R (which can be graphically represented by the intercepts of the lower and upper asymptotes, respectively, of the extended Hill plot with the *y*-axis at $\log P_{O_2}=0$). The diversity in regulatory mechanisms encountered in extracellular O_2-binding proteins calls for a parallel analysis of myriapod Hcs.

The diplopod *Archispirostreptus gigas* is a large, slow-moving, forest floor-dwelling deposit feeder from East Africa (Pechenik, 2005), which suggests it may have markedly different metabolic requirements from those of chilopods, which are fast-moving carnivores. As with insects, myriapods may have occludable spiracles and exhibit discontinuous gas exchange whereby their tissues may intermittently become hypoxic (Schmitz and Harrison, 2004). As soil dwellers they are moreover subjected to temporary flooding, which decreases O_2 availability. With the aim of gaining insight into the evolutionary origin of millipede Hc, its functional adaptations and its allosteric regulatory mechanisms, we investigated the primary structure of *A. gigas* Hc and its O_2-binding properties in the native hemolymph and Hc solutions under differing physico-chemical conditions as regards pH, (L)-lactate and divalent cation concentrations.

MATERIALS AND METHODS

Animals and hemolymph

Specimens of the giant millipede *A. gigas* (Peters 1855) weighing 25–82 g were obtained from a dealer (Exotera GmbH, Holzheim, Germany), and kept in a terrarium at room temperature and fed regularly.

Hemolymph for O_2-binding studies was drawn from 12 animals using a hypodermic syringe fitted with 23 gauge × 1¼ in needles to pierce the dorsal intersegmental membranes. All subsequent preparative steps were carried out at 0–4°C. The samples were pooled, and centrifuged for 10 min at 10,000 ***g*** to remove cellular debris. Samples used to record extended Hill plots (see below) were concentrated by ultrafiltration in Amicon Ultra Centrifugal filters (cut-off: 100,000 kDa; Millipore, Billerica, MA, USA). To study the effect of cations (Na^+, Ca^{2+}, Mg^{2+}), the hemolymph was dialyzed against three changes of 10 mmol l^{-1} Tris-HCl buffer, pH 7.5 at a 1:300 sample:buffer ratio and concentrated. The dialyzed hemolymph is denoted as 'stripped Hc'. The hemolymph and Hc preparations were divided into 100 µl aliquots that were stored at −80°C and thawed individually for measurement of O_2 equilibria.

Hc concentration was derived from the absorbance at 335 nm using the ε=0.0175 l mol^{-1} cm^{-1} reported for crab *Carcinus manaes* Hc (Nickerson and Van Holde, 1971; Weber et al., 2008) and a subunit mass of 73.5 kDa as deduced from cDNA sequence analysis (described below).

Protein biochemistry

A polyclonal antibody was generated against purified *A. gigas* Hc in guinea pigs. SDS-PAGE was performed on a 7.5% gel using standard methods as previously described (Jaenicke et al., 1999). Two-dimensional gel electrophoresis (2D-PAGE) using pH 3.5–10 ampholines was performed according to O'Farrell (O'Farrell, 1975). For western blotting, the proteins were transferred to nitrocellulose at 0.8 mA cm^{-2}. Non-specific binding sites were blocked by 5% non-fat dry milk in TBST (10 mmol l^{-1} Tris-HCl, pH 7.4, 140 mmol l^{-1} NaCl, 0.25% Tween-20). Incubation with the anti-Hc antibody in 5% non-fat dry milk/TBST was carried out for 2 h at room temperature. The filters were washed 3×10 min in TBST and subsequently incubated for 1 h with a goat anti-rabbit secondary antibody conjugated with alkaline phosphatase, diluted in 5% non-fat dry milk/TBST. The membranes were washed as above and detection was carried out using nitro-blue-tetrazolium and bromo-chloro-indolyl-phosphate.

Mass spectrometry was carried out by nanoLC-ESI-ion trap analysis after tryptic digest of the Hc bands from SDS-PAGE. Protein identification was performed with Mascot software (Perkins et al., 1999) using the NCBI nr database.

Cloning of *A. gigas* Hc cDNA

Total RNA was extracted from the whole animal after removal of the cuticle. Poly(A)$^+$ RNA was purified from total RNA using a PolyATract kit (Promega, Madison, WI, USA); 5 µg poly(A)$^+$ RNA was then used for the construction of a directionally cloned cDNA expression library with the Lambda ZAP-cDNA synthesis kit (Stratagene, Agilent Technologies, Santa Clara, CA, USA). The library was screened with the anti-*A. gigas* Hc antibodies. Positive phage clones were converted to plasmid vectors using the material provided in the kit. The cDNAs inserted in the pBK-CMV vector were sequenced on both strands by a commercial sequencing service (Genterprise, Mainz, Germany). A full-length Hc cDNA sequence was obtained and is available from the EMBL/GenBank databases under the accession number HE574799.

Sequence and phylogenetic analyses

The web-based tools provided by the ExPASy Molecular Biology Server of the Swiss Institute of Bioinformatics (http://www.expasy.org) were used for sequence analyses. A multiple sequence alignment of the amino acid sequences of selected arthropod Hcs and phenoloxidases (supplementary material Table S1) was constructed with MAFFT 6 (Katoh et al., 2005) (http://mafft.cbrc.jp/alignment/server/). The L-INS-i routine and the BLOSUM 45 matrix were selected. The final alignment covered 93 sequences and 906 positions (supplementary material Fig. S1).

Bayesian phylogenetic analysis was performed using MrBayes 3.1.2 (Huelsenbeck and Ronquist, 2001). We assumed the WAG model with a gamma distribution of substitution rates. Metropolis-coupled Markov chain Monte Carlo (MCMCMC) sampling was performed with one cold and three heated chains. Two independent runs were performed in parallel for five-million generations. The average standard deviation of split frequencies was <0.005. Starting trees were random and the trees were sampled every 1000th generation. Posterior probabilities of the nodes were estimated on the final 4000 trees (burnin=1000).

Oxygen equilibrium measurements

O_2 equilibria were measured at 25°C using a modified gas-diffusion chamber (Weber, 1981) coupled to two serially linked precision Wösthoff gas mixing pumps (Bochum, Germany) for mixing pure (>99.998%) N_2 and atmospheric air. In the procedure, absorbance of 3 µl hemolymph samples was recorded at 365 nm following equilibration with pure O_2 and pure N_2 to obtain the full saturation range, and thereafter monitored during stepwise increases in the P_{O_2} of the equilibrating gas mixture. O_2 equilibrium curves were derived as the relationship between absorbance levels (corresponding to O_2 saturation) and calculated O_2 tensions at the individual steps. In order to assess the Bohr effect, pH values in the measured samples were varied by adding 1 mol l^{-1} Tris-HCl (for measurements at >pH 7) or bisTris buffers (<pH 7) to obtain a final buffer concentration of 0.1 mol l^{-1} (unless otherwise indicated). The pH values were measured at 25°C using a BMS 2 MK 2 microelectrode coupled to a PHM 64 Research pH meter (Radiometer, Copenhagen, Denmark).

For each O_2 equilibrium curve, P_{50} and n_{50} values (O_2 tension and Hill's cooperativity coefficients, respectively, at 50% oxygenation) were derived from the zero intercepts and slopes, respectively, of Hill plots ($\log S/(1–S)$ *versus* $\log P_{O_2}$, where S is the fractional saturation) based on at least four equilibrium steps in the 25–75% saturation range. Extended Hill plots for assessment of K_T, K_R and other allosteric parameters were obtained by recording at least 10 additional steps at low (<10%) and high (>90%) O_2 saturations.

The oxygen fractional saturation, S, at each step was derived as:

$$S = \frac{A - A_0}{A_{100} - A_0} , \quad (1)$$

where A is the absorbance at each step, and A_{100} and A_0 are the absorbance recorded with pure O_2 and pure N_2, respectively.

The allosteric parameters were obtained by fitting the MWC 'two-state, concerted' model (Monod et al., 1965) to the data by non-linear least squares curve fitting according to the equation:

$$S = \frac{LK_T P_{O_2}(1 + K_T P_{O_2})^{q-1} + K_R P_{O_2}(1 + K_R P_{O_2})^{q-1}}{L(1 + K_T P_{O_2})^q + (1 + K_R P_{O_2})^q} , \quad (2)$$

where S denotes the fractional saturation, L is the allosteric constant ([T]/[R]) in the absence of ligand, P_{O_2} is the partial pressure of O_2, and q denotes the number of interacting binding sites. To minimize errors introduced by incomplete saturation or desaturation when equilibrating with pure O_2 or N_2, respectively, the true absorbance at zero and full saturation was found in a single fitting procedure, along with the allosteric parameters including P_m and n_{max} (see Table 1), as described previously (Fago et al., 1997). The Bohr factor (φ, the number of protons released per O_2 molecule bound) was calculated from the slope of $\log P_{50}$ as a function of pH:

$$\varphi = \frac{\Delta \log(P_{50})}{\Delta \mathrm{pH}} . \quad (3)$$

RESULTS AND DISCUSSION

Molecular characterization of *A. gigas* Hc

SDS-PAGE and 2D-PAGE followed by western blotting employing specific anti-Hc antibodies identified two distinct Hc subunits in the hemolymph of *A. gigas* (Fig. 1). Mass spectrometry (nanoLC-ESI-ion trap) showed that the two bands corresponded to the same Hc subunit and identified several glycosylated peptides. A single Hc cDNA sequence was obtained by screening an *A. gigas* cDNA expression library. No additional subunit could be detected despite extensive screening and additional RT-PCR experiments with the ESTs of this species (Meusemann et al., 2010). Thus, in contrast to most arthropod Hcs (Markl and Decker, 1992; Kusche et al., 2003), the native *A. gigas* Hc likely consists of only a single subunit type.

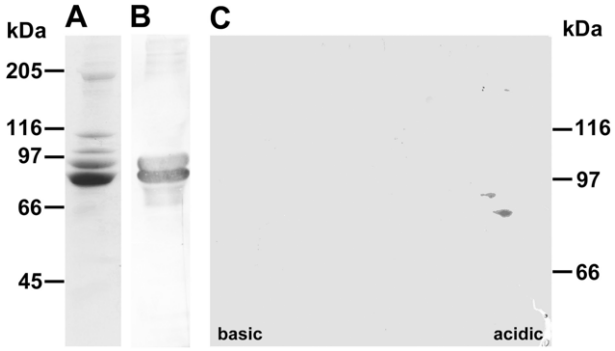

Fig. 1. Identification of *Archispirostreptus gigas* hemocyanin (Hc). (A) Total hemolymph proteins were separated on SDS-PAGE and stained with Coomassie Brilliant Blue R-250. (B) Western blot analysis with specific anti-*A. gigas* Hc antibodies identified two bands of around 75 kDa. (C) Hemolymph proteins were separated by 2D-PAGE and the Hc subunits were detected by western blotting. The molecular mass markers are indicated.

The full-length Hc cDNA sequence encompasses 2115 bp (plus a polyA tail of 18 bp), including an open reading frame of 1962 bp beginning with a methionine ATG at bp 40 (supplementary material Fig. S1). The typical polyadenylation signal AATAAA is located 34 bp upstream of the start of the polyA tail. A polypeptide of 653 amino acids was deduced. The predicted molecular mass was 75.2 kDa. The N-terminal sequence harbors a typical signal peptide of 17 amino acids (supplementary material Fig. S1). Thus, the native secreted Hc subunit comprises 636 amino acids with a calculated molecular mass of 73.5 kDa. Three putative *N*-glycosylation sites were detected at amino acid positions 404, 435 and 630. Their usage is supported by the glycosylated peptides detected in mass spectrometry. Differential glycosylation most likely explains the two Hc bands detected in the western blot.

Archispirostreptus gigas Hc is most similar to the Hc of the diplopod *Spirostreptus* sp. (Kusche and Burmester, 2001), with which it shares 94.0% of the amino acids and 95.3% of the nucleotides in the coding region. The six copper-coordinating histidines that are strictly conserved in all arthropod Hcs (Burmester, 2002; Linzen et al., 1985) are present in the copper-binding sites A and B. The amino acid sequence of *A. gigas* Hc was included in a multiple sequence alignment of a total of 86 other Hcs from all arthropod subphyla. Six phenoloxidase sequences were added as an outgroup. Bayesian phylogenetic analyses support the monophyly of the myriapod (diplopod and chilopod) Hcs (posterior probability: 1.0; Fig. 2). The *A. gigas* Hc groups with the *Spirostreptus* sp. Hc. The two diplopod Hcs are a sister group of the HcA subunit of *Scutigera coleoptrata* (Kusche et al., 2003), while the other four

Table 1. The derived MWC parameters for O_2 equilibria at 25°C in the presence and absence of added (L)-lactate and Ca^{2+}

	T (°C)	pH	[(L)-lactate] (mmol l^{-1})	[Ca^{2+}] (mmol l^{-1})	P_m (mmHg)	P_{50} (mmHg)	n_{50}	n_{max}	K_T ($mmHg^{-1}$)	K_R ($mmHg^{-1}$)	c	ΔG (kJ mol^{-1})	q	log$L$
Hemolymph	25	7.841	0	0	4.00	3.76	1.77	1.82	0.0724	0.516	0.140	4.54	5.30±3.2	1.66±0.87
Hemolymph	25	7.857	10	0	4.68	5.02	2.21	2.25	0.111	0.495	0.225	3.69	10.7±6.2	3.89±1.8
Hemolymph	25	6.850	0	0	26.6	27.8	2.13	2.24	0.0182	0.104	0.175	4.28	8.08±3.8	3.58±0.45
Stripped Hc	25	7.995	0	0	25.6	24.7	1.32	–*	0.0233	0.193	0.121	2.81	3.01±24	2.19±36
Stripped Hc	25	7.960	0	20	4.67	5.02	1.68	1.69	0.106	0.681	0.156	4.18	5.00±4.1	2.52±0.74

Hc, hemocyanin; P_m, median O_2 tension; P_{50}, O_2 tension at 50% oxygenation; n_{50}, Hill's cooperativity coefficient at 50% oxygenation; n_{max}, maximal cooperativity coefficient; K_T and K_R, oxygen dissociation constants for the tense state and relaxed state, respectively; $c=K_T/K_R$; ΔG, free energy of cooperativity; q, the number of interacting O_2-binding sites; and L, allosteric constant.

*Could not be determined in the data fitting.

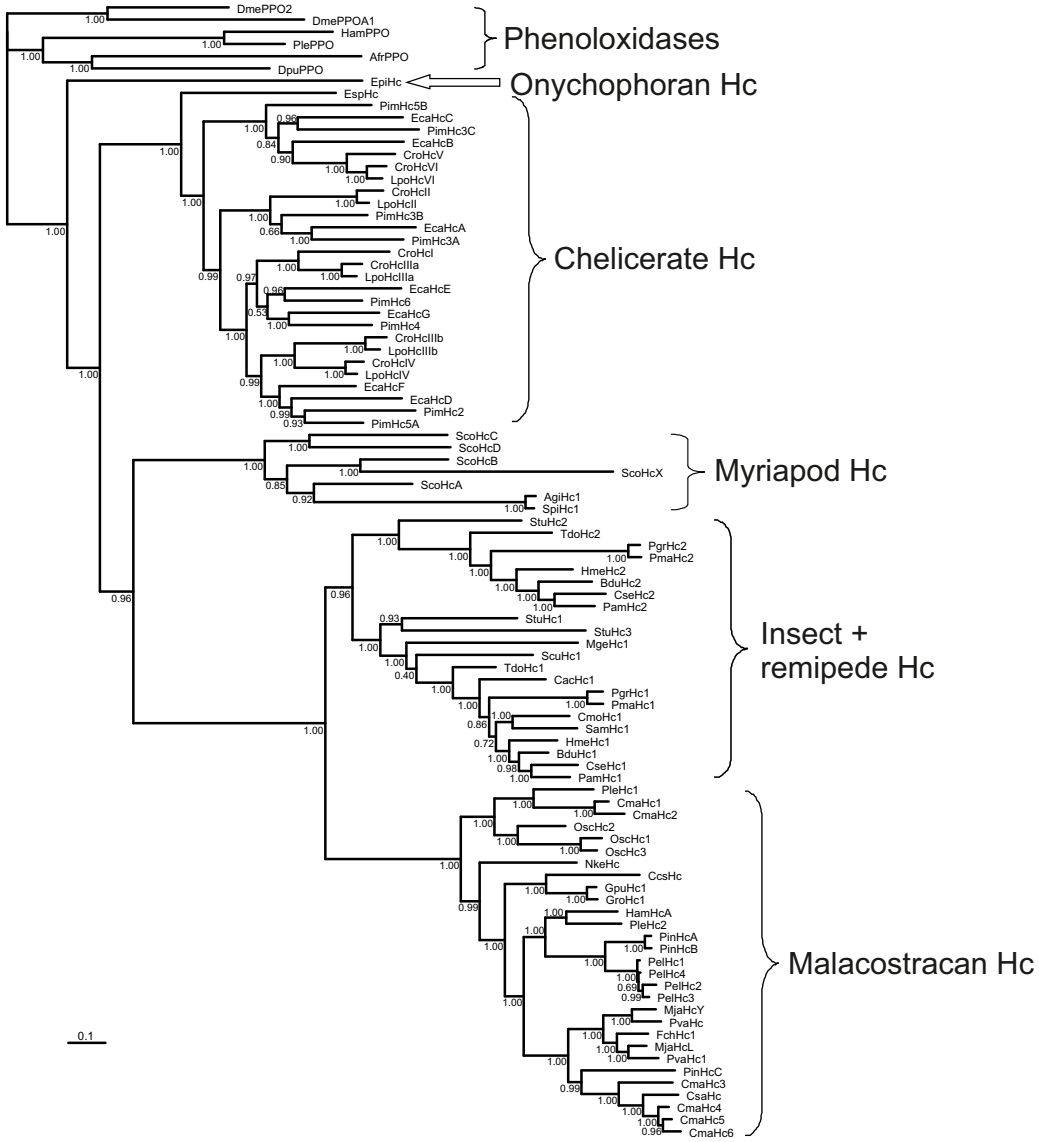

Fig. 2. Bayesian phylogenetic analysis of the arthropod Hcs. The numbers beside the branches represent Bayesian posterior probabilities. The bar represents 0.1 PAM (point accepted mutation) distance. See supplementary material Table S1 for abbreviations.

subunits of *S. coleoptrata* are basal. This demonstrates an early divergence of distinct subunit types in the myriapods before the separation of Diplopoda and Chilopoda, which occurred at least ~420 million years ago in the Silurian period (Wilson and Anderson, 2004). Thus, the formation of the oligohexameric Hc (probably a 36-mer) is an ancient event. The phylogeny of the Hc subunits further supports a monophyly of the Mandibulata (Myriapoda + Crustacea; 0.96 support), but rejects Myriochelata (Myriapoda + Chelicerata).

Oxygen binding

Archispirostreptus gigas whole hemolymph contains high levels of Hc (159 mg ml^{-1}) compared with centipedes (93 mg ml^{-1} in *Scutigera coleoptrata*) (Mangum et al., 1985). The whole hemolymph (Fig. 3) exhibits a high O_2 affinity [P_{50}=3.45 mmHg (0.46 kPa) at pH 8.1 and 25°C] compared with other crustacean Hcs studied under similar temperature and pH conditions (P_{50}=2.8–24 mmHg) (Morris and Bridges, 1994). The cooperativity coefficients are low (~1.5 at <pH 7.0 and >pH 8.0) but increase to ~3.0 near pH 7.4 (Fig. 3), a pattern commonly observed in other Hcs (Miller and Van Holde, 1974; Miller and Mangum, 1988). These O_2-binding properties differ sharply from those of centipedal *S. coleoptrata* Hc, despite similar quaternary structures and subunit sequence homology in millipede and centipede Hcs (supplementary material Fig. S1). The high O_2 affinity and low cooperativity in *A. gigas* Hc predictably favor O_2 binding at low O_2 tensions, as expected to prevail in myriapods with gas-impermeable exoskeletons that lack the capacity for tracheal ventilation (Rajulu, 1970). This contrasts with the low affinity and high cooperativity observed in centipede *S. coleoptrata* Hc, which may be adaptive in enhancing O_2 release in the highly active centipedes (Markl et al., 2009; Jaenicke et al., 1999).

Interaction with allosteric cofactors

The O_2 affinity of whole *A. gigas* hemolymph was not materially affected by pH or by the addition of lactate or Ca^{2+} at <pH 6.7 (Fig. 3B). However, at pH 7.0–8.0, a marked Bohr factor (φ=–0.73) was observed that was further increased by effectors [φ=–0.77 and –0.85, respectively, in the presence of 10 mmol l^{-1} (L)-lactate and 20 mmol l^{-1} Ca^{2+}]. The marked Bohr effect implies that activity-induced acidification of tissues bathed by the hemolymph will enhance unloading of O_2 from the Hc. A similarly large Bohr effect (φ=–0.87) has been observed in the house centipede, *S. coleoptrata* (Mangum et al., 1985).

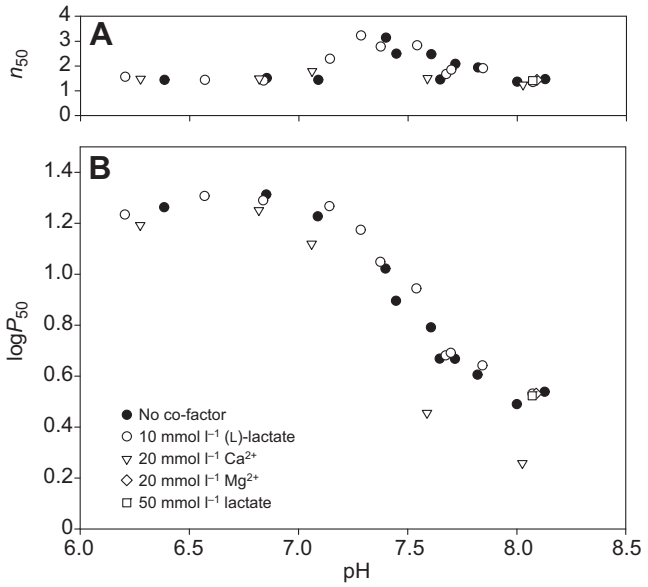

Fig. 3. The pH dependence of Hill's cooperativity coefficient (A) and O_2 tension (B) at 50% O_2-saturation (n_{50} and P_{50}, respectively) of *A. gigas* hemolymph at 25°C in the absence of added cofactors and in the presence of 10 mmol l^{-1} (L)-lactate, 20 mmol l^{-1} Ca^{2+}, 20 mmol l^{-1} Mg^{2+} and 50 mmol l^{-1} (L)-lactate.

In the intensively studied tetrametric vertebrate Hbs, the majority of the Bohr effect is attributable to oxygenation-linked binding of protons to surface His residues that increase their p*K* values (Lukin and Ho, 2004; Berenbrink, 2006). The subunits of *A. gigas* Hc contain 34 His residues, including the six copper-binding residues and four histidines in the interface between hexamers (H152, H155, H443 and H446) (supplementary material Fig. S1), and some of the free surface residues may undergo oxygenation-linked proton binding under physiological conditions and transmit forces during allosteric interaction (Markl et al., 2009), contributing to the Bohr effect. In tarantula *Eurypelma californicum* Hc, salt bridges between conserved surface histidine and glutamate residues located at particular intersubunit interfaces are considered responsible for the observed Bohr effect (Sterner and Decker, 1994). However, the mechanism of O_2 binding and its modulation by allosteric effectors depends on the interplay of many factors, including the coordination geometry and redox potential of copper. Studies on crustacean (*Panulirus interruptus* and *Carcinus aestuarii*) Hc suggest that the Bohr effect of arthropod Hcs results from pH-dependent structural modulation of the geometry of copper in the deoxygenated Hc molecules, 'leaving the question of identifying the role of individual amino acids to future studies' (Hirota et al., 2008).

Strikingly, the addition of 10 and 50 mmol l^{-1} (L)-lactate to whole hemolymph slightly decreased O_2 affinity in the range pH 7–8 (Fig. 3B), which contrasts sharply with the commonly encountered lactate-induced increase in O_2 affinity observed in crustacean Hcs, which would favor O_2 binding under hypoxic conditions (Truchot, 1980; Morris and Bridges, 1994; Bridges et al., 1984; Paoli et al., 2007; Hellmann et al., 2010).

The slight lactate effect observed in *A. gigas* supports the correlation between terrestrial life and reduced lactate effects reported in crustaceans – and extends it to diplopods. Accordingly, lactate has no effect on Hc–O_2 affinity in the tropical land hermit crab *Coenobita clypeoatus* (Morris and Bridges, 1986) and the terrestrial, obligate air-breathing decapod *Birgus latro* (Morris et al., 1988). Compared with marine crustaceans, Hc of the Christmas Island red landcrab, *Gecarcoides natalis*, even shows a reverse lactate effect [O_2 affinity falls with increasing (L)-lactate concentration] (Adamczewska and Morris, 1998) that predictably favors O_2 unloading in the tissues in terrestrial habitats where O_2 loading is secured.

Addition of Ca^{2+} ions to whole hemolymph drastically increased Hc–O_2 affinity in the pH range 7.0–8.0. The Ca^{2+} effect increased with pH (Fig. 3B) suggesting that the O_2-linked Ca^{2+}-binding sites become increasingly accessible and/or deprotonated with rising pH, as also observed in crustacean (*Penaeus monodon*) Hc (Beltramini et al., 2005). In contrast, addition of Mg^{2+} to whole hemolymph does not affect Hc–O_2 affinity, indicating that the O_2-linked cation-binding sites are specific to Ca^{2+} ions or that potential O_2-linked Mg^{2+}-binding sites are saturated in the whole hemolymph.

The pH of native hemolymph was 8.2 at 25°C, which falls within the range measured in freshly collected diplopod hemolymph (pH 8.0–8.5) (Xylander, 2009). This implies (see Fig. 3) that variations in Ca^{2+} concentration exert a tangible effect on O_2 affinity at physiological pH. The dose–response curve at ~pH 7.96 for the relationship between [Ca^{2+}] and P_{50} in stripped Hc (Fig. 4A), moreover, shows high sensitivity of P_{50} to Ca^{2+} at low cation levels that characterize arthropod hemolymph (3.5–4.3 mmol l^{-1} in arachnids) (Paul et al., 1994; Decker et al., 1980). Fitting the logP_{50}/[Ca^{2+}] curve to a hyperbola (Fig. 4A) indicates that the Ca^{2+} concentration required for half the maximum increase in logP_{50} – which reflects the apparent Ca^{2+} binding constant – is 12.3 mmol l^{-1}. The slope of the double logarithmic plot (Fig. 4B) of 0.55±0.05 (mean ± s.e.m.) reflects binding of 0.5–0.6 Ca^{2+} ions per O_2 molecule. In contrast to Ca^{2+}, 100 mmol l^{-1} Na^+ – the major cation in extracellular fluids – had no detectable effect on O_2 affinity of the stripped Hc (Fig. 4A) – supporting the view that the cation-binding site is highly specific for Ca^{2+}.

The exoskeleton of arthropods contains up to 40% mineral salts, predominantly calcium carbonate, that hardens the cuticle. Decreases in hemolymph pH associated with lactic acidoses under hypoxia may thus be expected to mobilize calcium carbonate from exoskeleton stores, raising hemolymph Ca^{2+} and stabilizing hemolymph pH. This scenario is analogous to that in turtles, whose shells are rich in calcium carbonate. In the painted turtle, *Chrysemys picta*, increases in lactic acid levels (up to 200 mmol l^{-1}) under anoxia are buffered largely by carbonate, resulting in the accumulation of calcium and lactate in the extracellular fluid or incorporation of calcium lactate into the shell (Jackson and Ultsch, 1982; Jackson, 2004). Our finding that Ca^{2+} increases Hc–O_2 affinity thus indicates that Ca^{2+} released under hypoxia will increase Hc–O_2 loading under these conditions.

Extended Hill plot analysis

The parameters obtained by fitting the MWC model to the data (Table 1) reveal close agreement between P_m and P_{50}, and between n_{max} and n_{50} values, reflecting highly symmetrical O_2 equilibrium curves, which permit analysis of allosteric effects in terms of changes in P_{50} values. In the absence of added effectors, the non-exclusive binding coefficient c in the hemolymph ($=K_T/K_R=0.14$), indicates an ~7-fold higher O_2 affinity in the relaxed than in the tense state.

The q values (5.3–10.7) suggest an interaction between at least 11 O_2-binding sites, indicating that cooperativity is not confined within the hexameric subunits but extends between the individual hexamers. Although the major structural elements are strictly conserved amongst arthropod Hcs (Markl and Decker, 1992; van Holde and Miller, 1995; Burmester, 2001), identification of the salt

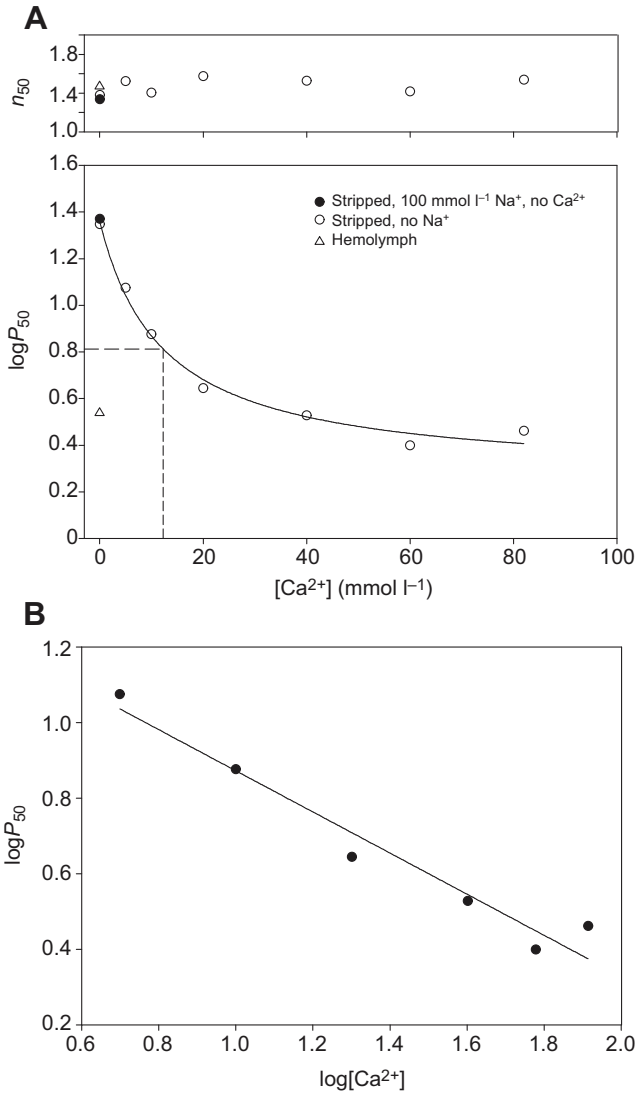

Fig. 4. (A) The effects of Ca^{2+} concentration on n_{50} and P_{50} of stripped *A. gigas* Hc at 25°C and pH 7.96±0.02 (mean ± s.d.) in the absence of added Na^+ and in the presence of 100 mmol l^{-1} Na^+ compared with the P_{50} and n_{50} values of the whole hemolymph. The dashed line indicates the [Ca^{2+}] where the O_2 affinity increase induced by Ca^{2+} is half-maximal. Hyperbolic regression: $\log P_{50}=1.36–1.10\times[Ca^{2+}]/(12.3+[Ca^{2+}])$. (B) Double logarithmic plot of P_{50} against [Ca^{2+}]. Linear regression: $\log P_{50}=1.42–(0.545\times\log[Ca^{2+}])+1.42$ (P=0.0008).

bridges implicated in inter-hexameric interactions is complicated by the large number of charged amino acid residues found in the five types of inter-hexamer interfaces (Markl et al., 2009). Given the large difference in cooperativity coefficients of the sluggish millipede *Spirostreptus* and the swift house centipede *S. coleoptrata* (n=1.3 and ~10, respectively), comparison of diplopod and chilopod Hcs promises insight into structure–function coupling.

Cooperativity between hexamers is accounted for by several salt bridges at inter-hexamer interfaces. Two salt bridges (Lys502 ↔ Asp575 and Asp567 ↔ Asn573) may act to connect the two 3×6mer half-molecules, and connections between adjacent hexamers may be stabilized by one salt bridge (Glu395 ↔ Lys628) (supplementary material Fig. S1) (Markl et al., 2009). The observation that q values exceeding 6 were only encountered in the hemolymph samples that had a higher Hc concentration than the stripped samples (2.43 and 1.70 mmol l^{-1}, respectively; Table 1) is congruent with dissociation of Hc subunits at low concentration (Svedberg and Heyroth, 1929). Analogously, the high q values found in the hemolymph at low pH and in the presence of lactate (q=10.7 and 8.08, respectively; Table 1) indicate that these conditions may favor the association of the hexameric subunits. The lower q value in stripped Hc, however, might also be due to the loss of other factors that are present in whole hemolymph, such as Ca^{2+}, which is known to increase the stability of the Hc quaternary structure (van Holde and Miller, 1995). Indeed, as shown in Table 1, addition of 20 mmol l^{-1} Ca^{2+} increases q of the stripped Hc from 3 to 5 and n_{50} from 1.32 to 1.68 (Table 1). This is in agreement with structural studies on diplopod Hc that show the presence of two opposing glutamate residue pairs (E410 and E411), which are not compensated by positively charged residues and might be responsible for the bridging of Ca^{2+} between hexameric subunits (Markl et al., 2009).

The slopes of unity seen at extremely low and high O_2 saturations in extended Hill plots (Fig. 5) reflect non-cooperative binding of the first and last O_2 molecules bound by the Hc molecules. As evidenced by the more than 2-fold increase in log$L$ upon addition of lactate (Table 1), lactate increases P_{50} by modulating the allosteric constant L, without affecting K_T and K_R (Fig. 5A). Contrasting with this, the Bohr effect is associated with a tangible decrease in K_T as well as K_R upon acidification (by >75% when hemolymph pH falls from ~7.8 to ~6.8; Table 1, Fig. 5A). Analogously, the drastically lower Hc–O_2 affinity in stripped Hc compared with that in the whole hemolymph (P_{50}=~26 and 4 mmHg, respectively, at pH ~7.9) results from marked reductions in both K_T and K_R (Table 1, Fig. 5B). Strikingly, addition of 20 mmol l^{-1} Ca^{2+} almost completely annuls these effects, resulting in left-shifting of the curve *via* increases in both K_T and K_R. The almost exact superimposition of the plot of stripped Hc in the presence of 20 mmol l^{-1} Ca^{2+} and of the whole hemolymph indicates that Ca^{2+} is the main physiological regulator of O_2 affinity in *A. gigas* Hc at constant pH.

O_2 equilibrium measurements were also carried out on stripped Hc in the presence and absence of 20 mmol l^{-1} Ca^{2+} at pH 6.4. However, it was not possible to fit the MWC model to these data because of the low level of cooperativity and almost identical K_T and K_R values, which suggests that the Hc molecules do not 'switch' between the T and R states and that Ca^{2+} does not exert an effect at low pH.

The mechanisms of allosteric control in *A. gigas* Hc differ strikingly from those characterizing the intensively studied vertebrate Hbs, where the major effectors (organic phosphates, chloride ions and protons) decrease Hb–O_2 affinity by lowering K_T, and other multimeric invertebrate O_2-binding proteins (other Hcs and extracellular Hbs). Thus in ~3000 kDa annelid (*Arenicola marina*, *Perineries aibuhitensis* and *Macrobdella decora*) Hbs and ~1750 kDa gastropod (*Biomphalaria glabrata*) Hb (Weber, 1981; Tsuneshige et al., 1989; Weber et al., 1995; Bugge and Weber, 1999) increased pH and divalent cation concentrations increase O_2 affinity predominantly by increasing K_R. The *A. gigas* Hc mechanism is moreover at variance with those encountered in other arthropod and in molluscan Hcs. Thus, as with multimeric Hbs, increased pH and divalent cation (Ca^{2+}) concentrations raise Hc–O_2 affinity of gastropod *Lymnea stagnalis* Hc predominantly by increasing K_R (Dawson and Wood, 1982), whereas Mg^{2+} ions raise K_R and lower K_T of *Haliotis iris* Hc (Behrens et al., 2002). The *A. gigas* Hc mechanism also differs from those observed in crustacean Hcs, where Mg^{2+} ions and increased pH increase O_2 affinity by raising K_R in *Callianassa californiensis* (Miller and Van Holde, 1974) and (L)-lactate increases Hc–O_2 affinity by increasing K_T *in Carcinus*

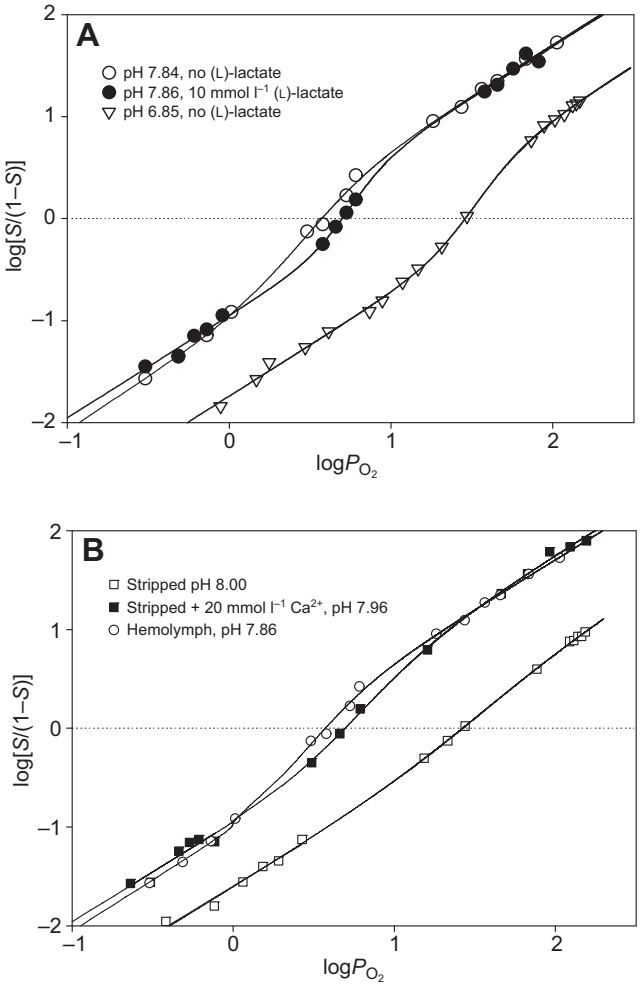

Fig. 5. (A) Extended Hill plots of *A. gigas* whole hemolymph measured at pH 6.85 and 7.84, and at pH 7.86 in the presence of 10 mmol l^{-1} (L)-lactate. (B) Plots of the stripped Hc at pH 8.00 in the absence and at pH 7.96 in the presence of 20 mmol l^{-1} Ca^{2+}, compared with that of the hemolymph at pH 7.86. The lines are MWC fits based on true saturation values.

maenas and *Callinectes sapidus* Hc (Weber et al., 2008; Johnson et al., 1988). Analyses of the allosteric interactions in terms of a nesting model that reveal hierarchies of interactions based on known hierarchy of subunit structure (Robert et al., 1987; Decker et al., 1988; Hellmann et al., 2003; Menze et al., 2005; Hellmann et al., 2008) will further elucidate the mechanisms regulating Hc–O_2 in myriapods.

CONCLUSIONS

Our study of *A. gigas* Hc shows that millipede Hcs are a sister group to centipede HcA, reflecting an early divergence of Hc subunits, which is associated with distinct differentiation in functional properties, notably in Hc–O_2 affinity and its regulation by protons (pH) and Ca^{2+} and lactate concentrations. The O_2-binding properties of the Hc are compatible with a role of the circulating hemolymph in complementing the tracheal system in supplying O_2 to the respiring tissues in myriapods. The pattern of allosteric effects observed in *A. gigas* Hc provides an ideal foundation for studies on the molecular basis and physiological significance of the variant patterns of allosteric control mechanisms encountered in multimeric gas-binding proteins.

LIST OF SYMBOLS AND ABBREVIATIONS

A	absorbance
c	non-exclusive binding coefficient K_T/K_R
Hb	hemoglobin
Hc	hemocyanin
K_R	relaxed (R)-state association equilibrium constant for O_2 binding
K_T	tense (T)-state association equilibrium constant for O_2 binding
L	allosteric constant ([T]/[R]) at zero oxygenation
n_{50}	Hill's cooperativity coefficient at half-saturation
n_{max}	maximal cooperativity coefficient
P_{50}	oxygen tension at half saturation
P_m	median oxygen tension
P_{O_2}	partial pressure of oxygen
q	number of interacting binding sites
S	apparent saturation
ΔG	free energy of cooperativity
φ	Bohr factor ($\Delta\log P_{50}/\Delta$pH)

ACKNOWLEDGEMENTS

We thank Anny Bang (Aarhus) and Christian Pick (Hamburg) for technical assistance and help with data handling. We thank Marcel Kwiatkowski (Hamburg) for the nanoLC-ESI-ion trap analysis.

AUTHOR CONTRIBUTIONS

Conception and design of the investigation: T.B., R.E.W. and A.F.; cloning and sequencing: S.H.-H.; oxygen equilibrium determinations: C.D.; protein biochemistry and phylogenetic analysis: T.B.; modeling studies: H.M.; integration and interpretation of the results and preparation of the manuscript: C.D., R.W., T.B. and A.F.

COMPETING INTERESTS

No competing interests declared.

FUNDING

The research was supported by grants from the Danish Council for Independent Research, Natural Sciences [grant no. 10-084565], the German Research Foundation [DFG grant no. Bu 965/9] and the Faculty of Science and Technology of Aarhus University.

REFERENCES

Adamczewska, A. M. and Morris, S. (1998). The functioning of the haemocyanin of the terrestrial Christmas Island red crab *Gecarcoidea natalis* and roles for organic modulators. *J. Exp. Biol.* **201**, 3233-3244.
Behrens, J. W., Elias, J. P., Taylor, H. H. and Weber, R. E. (2002). The archaeogastropod mollusc *Haliotis iris*: tissue and blood metabolites and allosteric regulation of haemocyanin function. *J. Exp. Biol.* **205**, 253-263.
Beltramini, M., Colangelo, N., Giomi, F., Bubacco, L., Di Muro, P., Hellmann, N., Jaenicke, E. and Decker, H. (2005). Quaternary structure and functional properties of *Penaeus monodon* hemocyanin. *FEBS J.* **272**, 2060-2075.
Berenbrink, M. (2006). Evolution of vertebrate haemoglobins: histidine side chains, specific buffer value and Bohr effect. *Respir. Physiol. Neurobiol.* **154**, 165-184.
Bonaventura, J. and Bonaventura, C. (1980). Hemocyanins: relationships in their structure, function and assembly. *Amer. Zool.* **20**, 7-17.
Bridges, C. R., Morris, S. and Grieshaber, M. K. (1984). Modulation of haemocyanin oxygen affinity in the intertidal prawn *Palaemon elegans* (Rathke). *Respir. Physiol.* **57**, 189-200.
Brouwer, M. and Serigstad, B. (1989). Allosteric control in *Limulus polyphemus* hemocyanin: functional relevance of interactions between hexamers. *Biochemistry* **28**, 8819-8827.
Bugge, J. and Weber, R. E. (1999). Oxygen binding and its allosteric control in hemoglobin of the pulmonate snail, *Biomphalaria glabrata. Am. J. Physiol.* **276**, R347-R356.
Burmester, T. (2001). Molecular evolution of the arthropod hemocyanin superfamily. *Mol. Biol. Evol.* **18**, 184-195.
Burmester, T. (2002). Origin and evolution of arthropod hemocyanins and related proteins. *J. Comp. Physiol. B* **172**, 95-107.
Dawson, A. and Wood, E. J. (1982). Equilibrium and kinetic studies of oxygen binding to the haemocyanin from the freshwater snail *Lymnaea stagnalis. Biochem. J.* **207**, 145-153.
Decker, H., Schmid, R., Markl, J. and Linzen, B. (1980). Hemocyanins in spiders, XII. Dissociation and reassociation of *Eurypelma* hemocyanin. *Hoppe Seylers Z. Physiol. Chem.* **361**, 1707-1717.
Decker, H., Connelly, P. R., Robert, C. H. and Gill, S. J. (1988). Nested allosteric interaction in tarantula hemocyanin revealed through the binding of oxygen and carbon monoxide. *Biochemistry* **27**, 6901-6908.
Fago, A., Bendixen, E., Malte, H. and Weber, R. E. (1997). The anodic hemoglobin of *Anguilla anguilla*. Molecular basis for allosteric effects in a root-effect hemoglobin. *J. Biol. Chem.* **272**, 15628-15635.

Hellmann, N., Weber, R. E. and Decker, H. (2003). Nested allosteric interactions in extracellular hemoglobin of the leech *Macrobdella decora*. *J. Biol. Chem.* **278**, 44355-44360.
Hellmann, N., Weber, R. E. and Decker, H. (2008). Linked analysis of large cooperative, allosteric systems: the case of the giant HBL hemoglobins. In *Methods in Enzymology: Globins and Other Nitric Oxide-Reactive Proteins Part A* (ed. R. K. Poole), pp. 463-485. London: Academic Press.
Hellmann, N., Paoli, M., Giomi, F. and Beltramini, M. (2010). Unusual oxygen binding behavior of a 24-meric crustacean hemocyanin. *Arch. Biochem. Biophys.* **495**, 112-121.
Hirota, S., Kawahara, T., Beltramini, M., Di Muro, P., Magliozzo, R. S., Peisach, J., Powers, L. S., Tanaka, N., Nagao, S. and Bubacco, L. (2008). Molecular basis of the Bohr effect in arthropod hemocyanin. *J. Biol. Chem.* **283**, 31941-31948.
Huelsenbeck, J. P. and Ronquist, F. (2001). MRBAYES: Bayesian inference of phylogenetic trees. *Bioinformatics* **17**, 754-755.
Jackson, D. C. (2004). Surviving extreme lactic acidosis: the role of calcium lactate formation in the anoxic turtle. *Respir. Physiol. Neurobiol.* **144**, 173-178.
Jackson, D. C. and Ultsch, G. R. (1982). Long-term submergence at 3°C of the turtle, *Chrysemys picta bellii*, in normoxic and severely hypoxic water: II. Extracellular ionic responses to extreme lactic acidosis. *J. Exp. Biol.* **96**, 29-43.
Jaenicke, E., Decker, H., Gebauer, W. A., Markl, J. and Burmester, T. (1999). Identification, structure, and properties of hemocyanins from Diplopod myriapoda. *J. Biol. Chem.* **274**, 29071-29074.
Johnson, B. A., Bonaventura, C. and Bonaventura, J. (1988). Allostery in *Callinectes sapidus* hemocyanin: cooperative oxygen binding and interactions with L-lactate, calcium, and protons. *Biochemistry* **27**, 1995-2001.
Katoh, K., Kuma, K., Toh, H. and Miyata, T. (2005). MAFFT version 5: improvement in accuracy of multiple sequence alignment. *Nucleic Acids Res.* **33**, 511-518.
Keilin, D. and Wang, Y. L. (1946). Haemoglobin of *Gastrophilus* larvae. Purification and properties. *Biochem. J.* **40**, 855-866.
Kusche, K. and Burmester, T. (2001). Diplopod hemocyanin sequence and the phylogenetic position of the myriapoda. *Mol. Biol. Evol.* **18**, 1566-1573.
Kusche, K., Ruhberg, H. and Burmester, T. (2002). A hemocyanin from the Onychophora and the emergence of respiratory proteins. *Proc. Natl. Acad. Sci. USA* **99**, 10545-10548.
Kusche, K., Hembach, A., Hagner-Holler, S., Gebauer, W. and Burmester, T. (2003). Complete subunit sequences, structure and evolution of the 6 x 6-mer hemocyanin from the common house centipede, *Scutigera coleoptrata*. *Eur. J. Biochem.* **270**, 2860-2868.
Linzen, B., Soeter, N. M., Riggs, A. F., Schneider, H. J., Schartau, W., Moore, M. D., Yokota, E., Behrens, P. Q., Nakashima, H., Takagi, T. et al. (1985). The structure of arthropod hemocyanins. *Science* **229**, 519-524.
Loewe, R. (1978). Hemocyanins in spiders. *J. Comp. Physiol. A* **128**, 161-168.
Lukin, J. A. and Ho, C. (2004). The structure–function relationship of hemoglobin in solution at atomic resolution. *Chem. Rev.* **104**, 1219-1230.
Mangum, C. P., Scott, J. L., Black, R. E., Miller, K. I. and Van Holde, K. E. (1985). Centipedal hemocyanin: its structure and its implications for arthropod phylogeny. *Proc. Natl. Acad. Sci. USA* **82**, 3721-3725.
Markl, J. and Decker, H. (1992). Molecular structure of the arthropod hemocyanins. *Adv. Comp. Environ. Physiol.* **13**, 325-376.
Markl, J., Moeller, A., Martin, A. G., Rheinbay, J., Gebauer, W. and Depoix, F. (2009). 10-A cryoEM structure and molecular model of the Myriapod (Scutigera) 6x6mer hemocyanin: understanding a giant oxygen transport protein. *J. Mol. Biol.* **392**, 362-380.
Menze, M. A., Hellmann, N., Decker, H. and Grieshaber, M. K. (2005). Allosteric models for multimeric proteins: oxygen-linked effector binding in hemocyanin. *Biochemistry* **44**, 10328-10338.
Meusemann, K., von Reumont, B. M., Simon, S., Roeding, F., Strauss, S., Kück, P., Ebersberger, I., Walzl, M., Pass, G., Breuers, S. et al. (2010). A phylogenomic approach to resolve the arthropod tree of life. *Mol. Biol. Evol.* **27**, 2451-2464.
Miller, K. I. and Mangum, C. P. (1988). An investigation of the nature of Bohr, Root, and Haldane effects in *Octopus dofleini* hemocyanin. *J. Comp. Physiol. B* **158**, 547-552.
Miller, K. and Van Holde, K. E. (1974). Oxygen binding by *Callianassa californiensis* hemocyanin. *Biochemistry* **13**, 1668-1674.
Monod, J., Wyman, J. and Changeux, J.-P. (1965). On the nature of allosteric transitions: a plausible model. *J. Mol. Biol.* **12**, 88-118.
Morris, S. and Bridges, C. R. (1986). Oxygen binding by the hemocyanin of the terrestrial hermit crab *Coenobita clypeatus* (Herbst) – the effect of physiological parameters in vitro. *Physiol. Zool.* **59**, 606-615.
Morris, S. and Bridges, C. R. (1994). Properties of respiratory pigments in bimodal breathing animals: air and water breathing by fish and crustaceans. *Amer. Zool.* **34**, 216-228.
Morris, S., Greenaway, P. and McMahon, B. R. (1988). Adaptations to a terrestrial existence by the robber crab *Birgus latro*. I. An *in vitro* investigation of blood gas transport. *J. Exp. Biol.* **140**, 477-491.
Nickerson, K. W. and Van Holde, K. E. (1971). A comparison of molluscan and arthropod hemocyanin – I. Circular dichroism and absorption spectra. *Comp. Biochem. Physiol.* **39B**, 855-872.
O'Farrell, P. H. (1975). High resolution two-dimensional electrophoresis of proteins. *J. Biol. Chem.* **250**, 4007-4021.
Paoli, M., Giomi, F., Hellmann, N., Jaenicke, E., Decker, H., Di Muro, P. and Beltramini, M. (2007). The molecular heterogeneity of hemocyanin: structural and functional properties of the 4x6-meric protein of *Upogebia pusilla* (Crustacea). *Gene* **398**, 177-182.
Paul, R. J., Pfeffer-Seidl, A., Efinger, R., Pörtner, H. O. and Storz, H. (1994). Gas transport in the haemolymph of arachnids. II. Carbon dioxide transport and acid–base balance. *J. Exp. Biol.* **188**, 47-63.
Pechenik, J. (2005) *Biology of the Invertebrates*. Boston, MA: McGraw-Hill.
Perkins, D. N., Pappin, D. J., Creasy, D. M. and Cottrell, J. S. (1999). Probability-based protein identification by searching sequence databases using mass spectrometry data. *Electrophoresis* **20**, 3551-3567.
Rajulu, G. S. (1969). Presence of haemocyanin in blood of a centipede *Scutigera longicornis* (chilopoda – Myriopoda). *Curr. Sci.* **38**, 168-169.
Rajulu, G. S. (1970). Tracheal pulsation in a marine centipede *Mixophilus indicus*. *Curr. Sci.* **39**, 397-398.
Robert, C. H., Decker, H., Richey, B., Gill, S. J. and Wyman, J. (1987). Nesting: hierarchies of allosteric interactions. *Proc. Natl. Acad. Sci. USA* **84**, 1891-1895.
Schmitz, A. and Harrison, J. F. (2004). Hypoxic tolerance in air-breathing invertebrates. *Respir. Physiol. Neurobiol.* **141**, 229-242.
Sterner, R. and Decker, H. (1994). Inversion of the Bohr effect upon oxygen binding to 24-meric tarantula hemocyanin. *Proc. Natl. Acad. Sci. USA* **91**, 4835-4839.
Svedberg, T. and Heyroth, F. H. (1929). The molecular weight of the hemocyanin of *Limulus polyphemus*. *J. Am. Chem. Soc.* **51**, 539-550.
Terwilliger, N. B. (1998). Functional adaptations of oxygen-transport proteins. *J. Exp. Biol.* **201**, 1085-1098.
Truchot, J.-P. (1980). Lactate increases the oxygen affinity of crab hemocyanin. *J. Exp. Zool.* **214**, 205-208.
Tsuneshige, A., Imai, K., Hori, H., Tyuma, I. and Gotoh, T. (1989). Spectrophotometric, electron paramagnetic resonance and oxygen binding studies on the hemoglobin from the marine polychaete *Perinereis aibuhitensis* (Grübe): comparative physiology of hemoglobin. *J. Biochem.* **106**, 406-417.
van Holde, K. E. and Miller, K. I. (1995). Hemocyanins. *Adv. Protein Chem.* **47**, 1-81.
van Holde, K. E., Miller, K. I. and Decker, H. (2001). Hemocyanins and invertebrate evolution. *J. Biol. Chem.* **276**, 15563-15566.
Weber, R. E. (1981). Cationic control of O_2 affinity in lugworm erythrocruorin. *Nature* **292**, 386-387.
Weber, R. E., Malte, H., Braswell, E. H., Oliver, R. W. A., Green, B. N., Sharma, P. K., Kuchumov, A. and Vinogradov, S. N. (1995). Mass spectrometric composition, molecular mass and oxygen binding of *Macrobdella decora* hemoglobin and its tetramer and monomer subunits. *J. Mol. Biol.* **251**, 703-720.
Weber, R. E., Behrens, J. W., Malte, H. and Fago, A. (2008). Thermodynamics of oxygenation-linked proton and lactate binding govern the temperature sensitivity of O_2 binding in crustacean (*Carcinus maenas*) hemocyanin. *J. Exp. Biol.* **211**, 1057-1062.
Wilson, H. M. and Anderson, L. I. (2004). Morphology and taxonomy of paleozoic millipedes (Diplopoda: Chilognatha: Archipolypoda) from Scotland. *J. Paleontol.* **78**, 169-184.
Wyman, J. (1969). Possible allosteric effects in extended biological systems. *J. Mol. Biol.* **39**, 523-538.
Xylander, W. E. R. (2009). Physico-chemical properties of haemolymph of Chilopoda and Diplopoda (Myriapoda, Arthropoda): protein content, pH, osmolarity. *Soil Org.* **81**, 431-439.